Scaling Laws for Light Absorption Enhancement Due to Nonrefractory Coating of Atmospheric Black Carbon Aerosol

Rajan K. Chakrabarty and William R. Heinson

Phys. Rev. Lett. **121**, 218701 — Published 19 November 2018

DOI: 10.1103/PhysRevLett.121.218701

Title: Scaling laws for Light Absorption Enhancement Due to Non-refractory Coating of Atmospheric Black Carbon Aerosol

Authors: Rajan K. Chakrabarty[1,2*] and William R. Heinson[1]

Affiliations:

[1]Center for Aerosol Science and Engineering, Department of Energy, Environmental and Chemical Engineering, Washington University in St. Louis, Missouri – 63130, USA.

[2]McDonnell Center for the Space Sciences, Washington University in St. Louis, Missouri – 63130, USA.

* Correspondence to*:* *chakrabarty@wustl.edu*

ABSTRACT

Black carbon (BC) aerosol, the strongest absorber of visible solar radiation in the atmosphere, contributes to a large uncertainty in direct radiative forcing estimates. A primary reason for this uncertainty is inaccurate parameterizations of BC mass absorption cross-section (MAC_{BC}) and its enhancement factor ($E_{MAC_{BC}}$)–resulting from internal mixing with non-refractory and non-light absorbing materials–in climate models. Here, applying scaling theory to numerically-exact electromagnetic calculations of simulated BC particles and observational data on BC light absorption, we show that MAC_{BC} and $E_{MAC_{BC}}$ evolve with increasing internal mixing ratios in simple power-law exponents of 1/3. Remarkably, MAC_{BC} remains inversely proportional to wavelength at any mixing ratio. When mixing states are represented using mass-equivalent core-shell spheres, as is done in current climate models, it results in significant under prediction of MAC_{BC}. We elucidate the responsible mechanism based on shielding of photons by a sphere's skin depth and establish a correction factor that scales with a ¾ power-law exponent.

Black carbon (BC) aerosol, emitted from anthropogenic and natural combustion processes, dominates the absorption of incoming shortwave solar radiation in the earth's atmosphere and is considered the second largest contributor to global warming after carbon dioxide [1,2]. In spite of its perceived importance in climate change, there exists a large discrepancy between model- and observation-based estimates of direct radiative forcing (DRF) by BC. Estimates of BC radiative forcing by the Intergovernmental Panel on Climate Change is comparable to that of methane, however, observational findings suggest these estimates to be conservative and could be higher [1,3-5]. A primary reason for this discrepancy could be attributed to the systematic underestimation of light absorption by BC, up to a factor of 3, in climate models compared to observationally-constrained estimates [3,4]. Current efforts to address this disagreement have been directed toward scaling up of BC mass absorption cross-sections (MAC_{BC})–defined as absorption cross-section per unit particle mass–in model parameterizations [1,6,7]. Accurate estimates of MAC_{BC} are critical for enabling models convert measured or modeled BC mass concentrations over a region to representative absorption coefficients, which serve as input parameter to radiative transfer algorithms [1].

The upward scaling of MAC_{BC} estimates in climate models has been motivated by recent field observations of BC existing in majority populations as internally mixed with non-refractory materials, including sulfate, nitrate, and organic carbon (OC) in the atmosphere [8-11]. Along with BC, combustion sources co-emit large amounts of volatile OC compounds, in addition to NO_x and SO_x, which upon undergoing atmospheric processing condense on BC particle surfaces as layers of external coating. These layers, which are typically non-absorbing in the visible solar spectrum, acts as "focusing lens" for the incoming light and results in an enhanced absorption cross-section or MAC_{BC} compared to that for an equivalent external mixture [10,12]. A broad

range of enhancement factors for MAC_{BC} (henceforth referred to as $E_{MAC_{BC}}$), from 1.05 to 3.5, has been observed during laboratory and field studies [9-11,13]. This large spread in $E_{MAC_{BC}}$ values accompanied by lack of any established scaling relationship makes it a cumbersome and challenging parameter to incorporate in models. A commonly adopted practice is, therefore, to either multiply uncoated MAC_{BC} values with a constant $E_{MAC_{BC}}$ or estimate approximate MAC_{BC} based on over-simplified aerosol models such as core-shell [7,14].

Here, we integrate results obtained from fractal modeling of internally-mixed BC and numerically-exact electromagnetic calculations with recent observational findings to establish universal scaling relationships for $E_{MAC_{BC}}$ and MAC_{BC} as a function of BC coating mass in the shortwave solar wavelengths (λ = 400 - 900 nm). Field and laboratory [8,9] data show that BC exists in the atmosphere primarily in three internally-mixed morphologies (figure 1): *bare aggregates* with point-contacting monomers, *partly coated aggregates* with monomer crevices filled with coating material but the aggregate not completely engulfed, and *embedded aggregates* with heavy coating mass and only the contours of the monomers evident. The dimensionless parameter $\frac{M_{total}}{M_{BC}}$ for a coated aggregate, defined as ratio of total particle mass (i.e., coating mass plus BC mass) to BC mass, ranges approximately between 1 and 5 for the partially coated, and $\geq$ 6 for the embedded types. Recent studies [9,13] have highlighted a particle's $\frac{M_{total}}{M_{BC}}$ as the primary parameter in controlling its $E_{MAC_{BC}}$. We show that when $E_{MAC_{BC}}$ and MAC_{BC} datasets are analyzed systematically as a function of $\frac{M_{total}}{M_{BC}}$, remarkable power-law scaling relations of the form $Y = Y_0 S^{\beta}$, where Y is either $E_{MAC_{BC}}$ or MAC_{BC}, S is either $\frac{M_{total}}{M_{BC}}$ or λ, and Y_0 is the prefactor and β is the power-law exponent, emerge. These simple scale dependencies would

enable climate models to accurately and inexpensively incorporate the absorption properties of BC in their parameterizations.

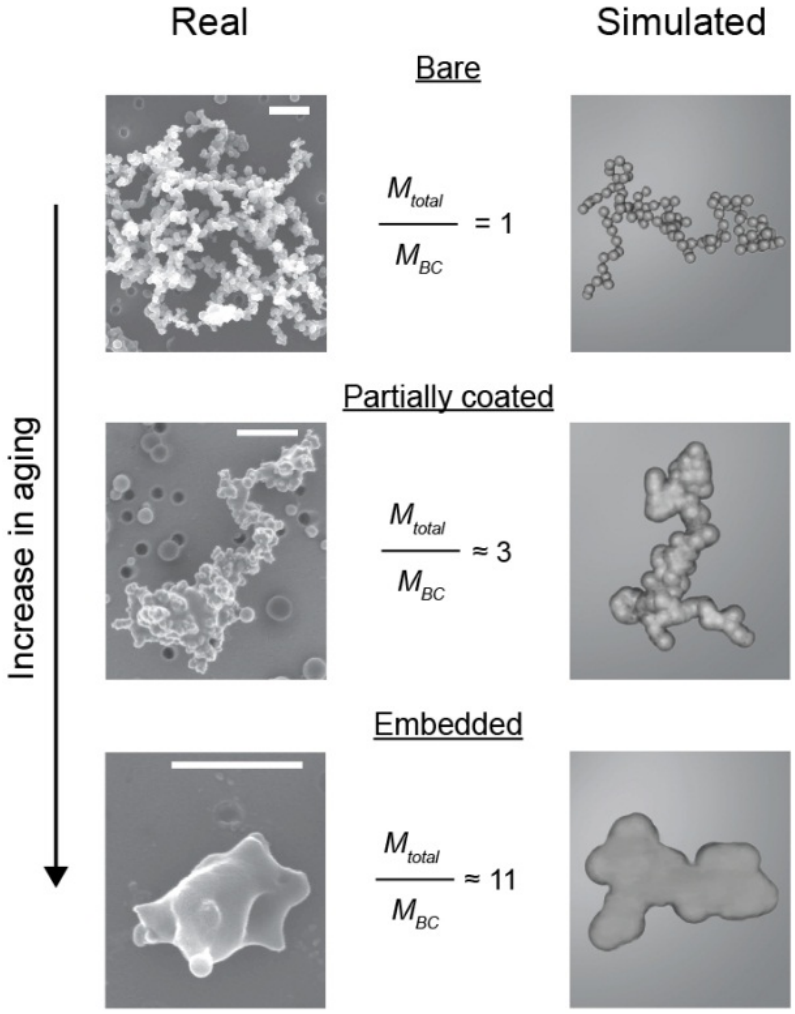

Figure 1: Morphologies of internally mixed black carbon (BC) aggregates. Three simulated aggregates from this study that were "cherry-picked" (shown in right column) demonstrates their close resemblance with real-world BC aerosol (left panel) corresponding to the three categories of internal mixing states as observed by China et al.[8]. The first row particles represent bare BC aggregate with point contacting monomers and an open fractal morphology; partially coated aggregates are shown in the second row; and thickly coated or embedded aggregates are displayed in the third row. The total particle mass to BC mass ratio is shown in the center for each class of particle.

We generated several hundred internally-mixed BC aggregates with $\frac{M_{total}}{M_{BC}}$ ranging between 1 and 18 using our recently published fractal aerosol model [15]. For this study, we used the materials densities for BC and non-refractory coating to be 1.8 and 1.2 g/cm^3, respectively [16,17]. The monomer diameter for bare BC aggregates was fixed at 25 nm and monomer number per aggregate ranged between 10 and 250 following past field observations. We applied the dipole-dipole approximation electromagnetic theory [18] to compute the orientationally-averaged MAC_{BC} and $E_{MAC_{BC}}$ for our simulated aggregates. Optical calculations were performed at three wavelengths λ=405nm, 532nm and 880nm, representing the near-UV, green, and red (near-IR) spectra of the incoming solar light. The complex indices of refraction for the BC monomers and refractory material coating were set at m=1.95-0.79i and 1.55-0i (no absorption), respectively [19-22]. This refractive index was chosen with the intention of making our findings applicable to broad-ranging scenarios of BC coated with OC and sulfates as found commonly occurring in the atmosphere.

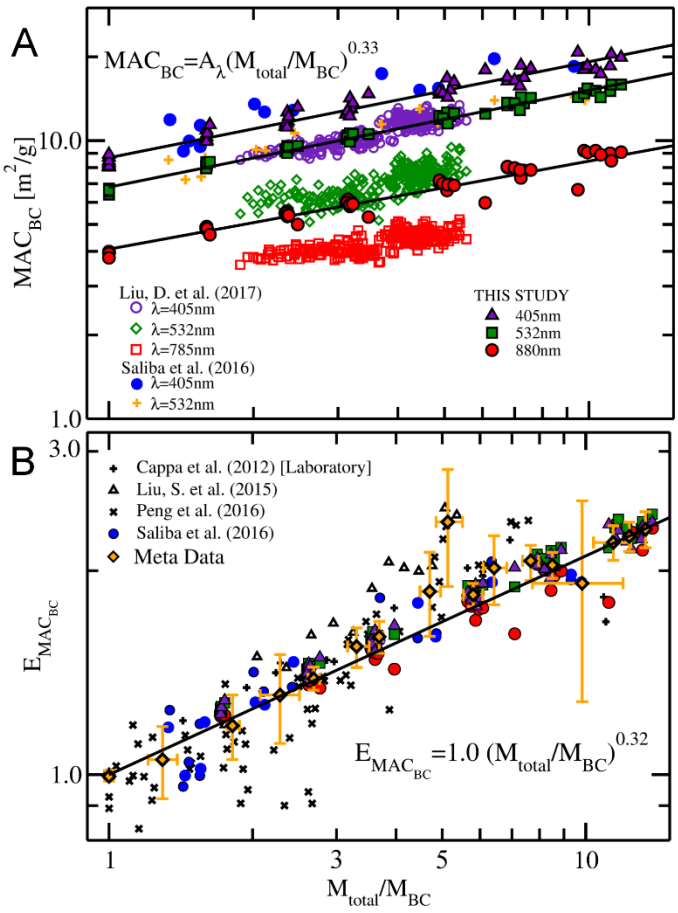

Figure 2: The 1/3 Scaling Laws for BC Mass Absorption Cross section (MAC_{BC}) and Enhancement of MAC_{BC} ($E_{MAC_{BC}}$). The MAC vs. total coated aggregate mass divided by its bare BC mass (M_{total}/M_{BC}) at wavelengths λ=405nm, 532nm, 880nm is shown in (A). At all λ, the MAC scales with a power law exponent of 0.33±0.05. Our work compares well to observational findings on cook stove emissions done by Saliba et al. [23], while data from Liu, D. et al. [13] has smaller prefactor owing to integrated absorption measurements as opposed to single-particle, yet their trends are parallel to the other data sets. (B). The enhancement of the absorption $E_{MAC_{BC}}$ of internally mixed BC is plotted versus $\frac{M_{total}}{M_{BC}}$. The "Meta Data" set of points represent the mean values of all observational dataset; the error bars represent two standard deviations. Independent of λ, $E_{MAC_{BC}}$ for all data sets follows the same upward increasing trend with a power-law exponent of 0.32±0.05. The $E_{MAC_{BC}}$ estimates from our simulation agrees very well (regression coefficient R^2 = 0.89) with findings from past observational field studies carried out globally [9-11,13]. This agreement suggests a universal behavior for $E_{MAC_{BC}}$ for internally mixed BC at visible and near infrared wavelengths.

In figure 2A, we compare the calculated MAC_{BC} versus $\frac{M_{total}}{M_{BC}}$ ratios for our aggregates with those reported by D. Liu et al. [13] and Saliba et al. [23]. D. Liu et al. performed a

comprehensive set of laboratory and ambient experiments investigating optical properties of combustion aerosols generated from automotive diesel engines, and a large number of intensive open wood fires and fireworks across the UK. They did not measure MAC_{BC} on a single particle level, instead estimated it from measurements of BC absorption coefficients–particle cross-sections integrated over a size distribution. Saliba and co-workers had coated freshly emitted BC aggregates from household cook stoves with secondary OC produced via the photo-oxidative ozonolysis of α-pinene. They measured MAC_{BC} on a single particle level using a single-particle soot photometer. All datasets follow very well the scaling relationship $MAC_{BC} = A_\lambda \left(\frac{M_{total}}{M_{BC}}\right)^{0.33\pm0.05}$, with the prefactor A_λ varying as $A_\lambda=3.6\lambda^{-0.98}$. Our MAC_{BC} for bare aggregates lie within the range of values reported for nascent soot by Bond et al. [1]. The variability in the prefactor A_λ with $\frac{M_{total}}{M_{BC}}$ could be attributed to differences in refractive indices and mass densities of coating materials, distributions in monomer sizes, and errors involved in the different measurement techniques. This is a multidimensional parameter space that needs to be explored in detail as part of future studies. For instance, the variation in mass densities of OC coating materials alone could range from 0.64 to 1.65 g/cm^3 and 1.06 to 1.45 g/cm^3 for biogenic and anthropogenic emissions, respectively [24]. Similarly, the variation in real part of *m* for OC aerosol could range from 1.36 to 1.66, while their imaginary part could have a non-zero and wavelength-dependent value [25].

In figure 2B, we show the universal scaling behavior of $E_{MAC_{BC}}$ as a function of $\frac{M_{total}}{M_{BC}}$ for all particles at the three wavelengths investigated in this study. Overlaid on our experimental results are observational datasets collected from different geographical regions. Peng et al.'s [11] data set, involving ambient carbonaceous aerosol collected in Houston (USA) and

Beijing (China) followed by oxidation in an environmental chamber, is representative of primarily internally mixed BC occurring in ambient urban conditions of developed and developing countries. Liu, S. et al.'s [9] dataset is from fossil fuel and residential biofuel emissions in and nearby London (UK), and also includes inter-continentally transported, atmospherically processed particles. Cappa et al. [10] provided laboratory measurements of $E_{MAC_{BC}}$, which are in agreement with our trends; however, their ambient findings on relatively smaller values of absorption enhancements for aged particles with substantial coatings present themselves as outliers (Fig. S1 in Supplemental Material). More recent studies [26-28] provide evidence for a combination of factors including off-centered coating or multiple inclusions of non-refractory materials on BC particle surface, and inefficient coating removal for aged aerosols using a thermodenuder operated at 225 °C that could have led to Cappa et al.'s observation of diminished $E_{MAC_{BC}}$ values.

In addition to the datasets corresponding to different studies, we included meta-analysis of all observational data, which in figure 2B is represented by the "Meta Data" set of points. As evident from the figure, the observational and meta dataset follow the scaling relation $E_{MAC_{BC}} = 1.0\left(\frac{M_{total}}{M_{BC}}\right)^{0.32\pm0.05}$, independent of variations in wavelength, with high coefficients of regression. For partially coated aggregates, $E_{MAC_{BC}}$ ranged from 1.3 to 1.9 while the embedded aggregates had $E_{MAC_{BC}}$ ranging between 2.2 and 2.5. It is imperative to disclose that data from a few more observational studies [29-31] could not be included in our analysis because of use of surrogate carbon materials to represent BC aerosol or unavailability of high resolution $\frac{M_{total}}{M_{BC}}$ measurements.

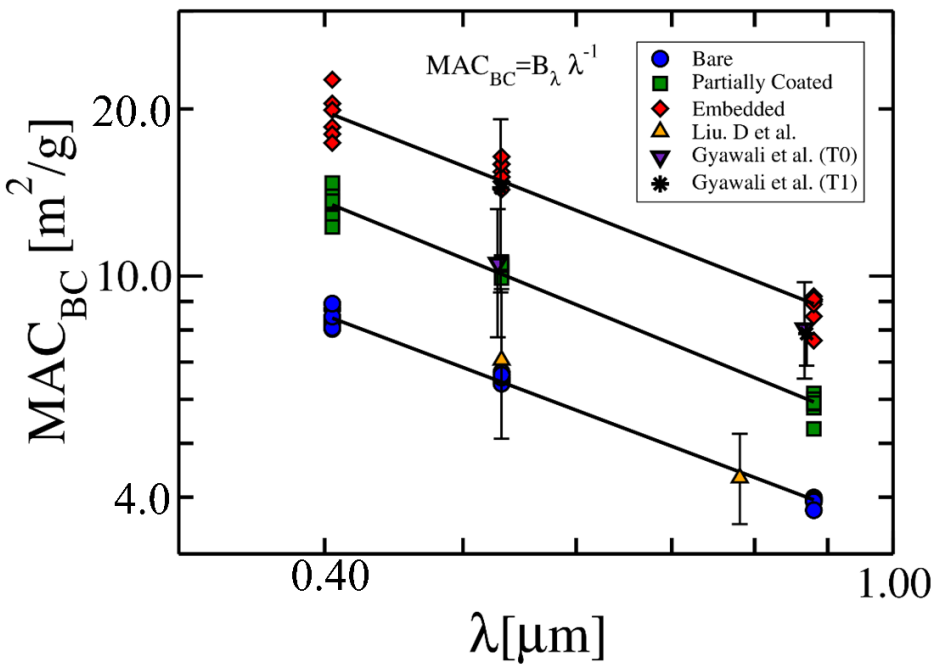

Figure 3: Inverse wavelength scaling of BC Mass Absorption Cross section (MAC_{BC}). The spectral response of MAC values for BC aggregates with varying degrees of mixing states are shown to follow an inverse functionality in wavelength (power law with exponent of -1). The fractal prefactor B_λ ranges from 3.5 (bare) to 5.2 (partially coated) to 7.8 (embedded), and denotes the enhancement in MAC_{BC} through the phenomenological "lensing effect". Observational datasets collected over California, USA (Gyawali et al.[32]) and Manchester, UK (Liu, D et al.[13]) follow the scaling trends. Error bars indicate the standard deviation in the reported measurements.

The wavelength dependence of MAC_{BC} for our aggregates exhibits a constant λ^{-1} power-law behavior (figure 3). Field datasets from Gyawali et al. [32] and Liu et al. [9] corroborates this constant scaling observation. Gyawali et al. characterized the evolution of multispectral optical properties of urban aerosols as they mixed with precursor gases and interacted with biogenic emissions during transportation to the forested Sierra Nevada foothills area in California. The power-law prefactor B_λ, however, increases as $3.6\left(\frac{M_{total}}{M_{BC}}\right)^{0.32}$ highlighting the enhanced focusing effect of the coating mass onto the BC core. The increased absorption cross-section of the BC core, owing to its fractal morphology, continues to exhibit Rayleigh optics behavior even at large values of $\frac{M_{total}}{M_{BC}}$ and R_g (ca. 450 nm).

The core's fractal morphology dictates the particle's phase shift parameter ρ to be always less than one, a necessary condition for the Rayleigh approximation to hold good [33,34]. ρ is directly proportional to the volume fraction of monomers in an aggregate and the Lorentz-Lorenz factor involving the imaginary index of refraction (*16, 26*). It quantifies how much phase shift the incoming light waves encounter across an aggregate compared to that in the absence of the particle. For sub-micron size BC aggregates, ρ scales with *Rg* as $\rho \approx R_g^{-0.2}$ (See Figs. S2 and S3 in Supplemental Material) implying a decreasing ρ with increasing aggregate size and its value remaining always less than 1. In the Rayleigh limit, the absorption cross-section of a BC aggregate could be simplistically calculated as $C_{abs} = N \cdot C_{abs,mono}$, where $C_{abs,mono} = 4\pi \frac{2\pi}{\lambda} a^3 Im\left(\frac{m^2-1}{m^2+2}\right)$ (where *Im* = imaginary part) is the absorption cross section of a monomer. The aggregate's MAC_{BC}, which is its C_{abs} divided by aggregate mass, then becomes equal to the mass absorption cross-section of a monomer: $MAC_{BC} = \frac{N \cdot C_{abs,mono}}{N \cdot m_{mono}} = \frac{C_{abs,mono}}{m_{mono}} = MAC_{mono}$, thus explaining its inverse scaling functionality with wavelength.

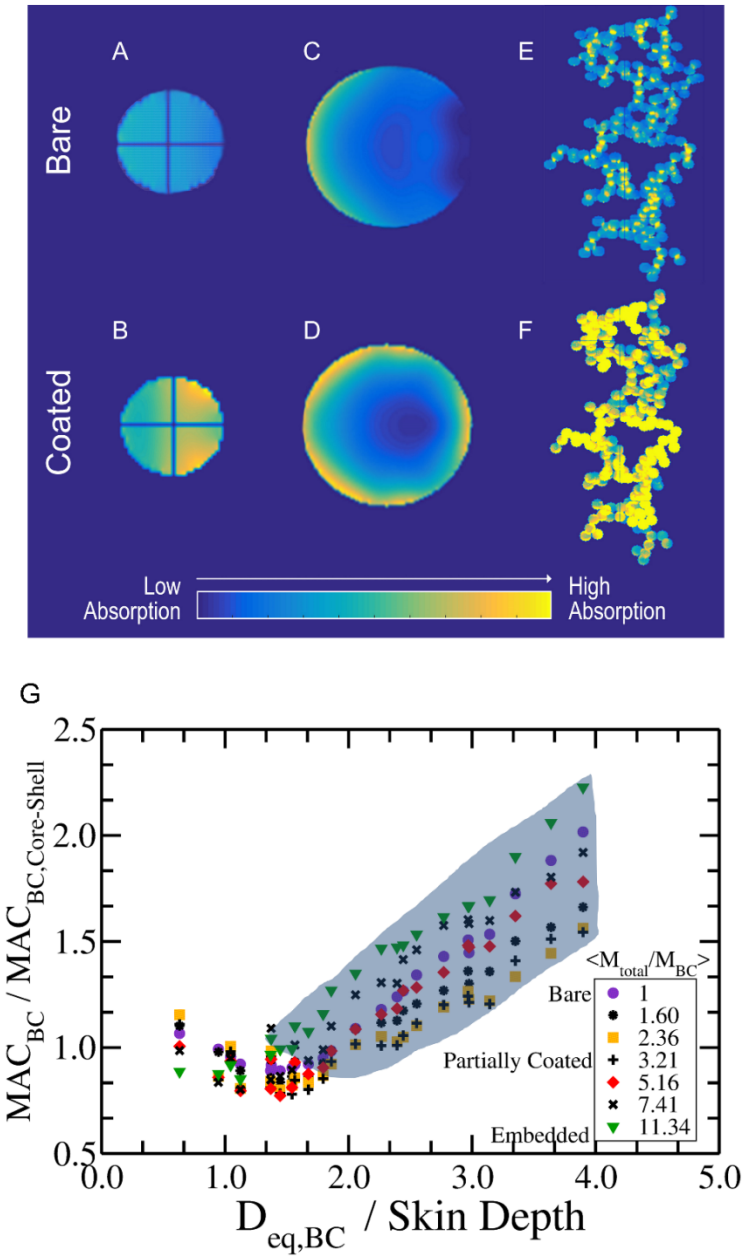

Figure 4: Role of Particle Morphology in Light Absorption. The strength of internal light absorption is shown for BC particles in their bare and heavily coated states (panels A-F). The coating material is non-absorbing and is therefore invisible in this representation. The incident light impacts the particles from the left. (A) BC sphere of diameter of D=80 nm; (B) Same sphere as (A) but having a 90 nm thick layer of coating; (C) BC sphere of D=300 nm; (D) Same sphere as (C) but with a 260 nm coating; and (E) and (F) represent BC aggregates having volume equivalence to spheres in (C) and (D), respectively. Particles (B), (D), and (F) are heavily coated which results in stronger absorption due to the "lensing effect." The diameter of spherical BC cores in (C) and (D) is larger than the absorption skin depth resulting in the interior of the particle being excluded from contributing to light absorption. The BC aggregate is porous in structure and therefore light penetrates completely into it

allowing the entire volume to add to the total absorption (panels E-F). (G) The MAC_{BC} ratios for coated aggregates to core-shell is plotted versus the mass equivalent sphere diameter $D_{eq,BC}$ divided by absorption skin depth. Significant disagreement is seen between the fractal and core-shell approximation models as $D_{eq,BC}$ becomes greater than the skin depth. As the equivalent spheres become larger than the absorption skin depth, the core-shell model underpredicts the MAC_{BC} of the aggregates. The shaded region scales as $\frac{MAC_{BC}}{MAC_{BC,Core-Shell}} \propto \left(\frac{D_{eq,BC}}{Skin\ Depth}\right)^{0.75}$

We computed mass-equivalent core-shell structure spheres of our coated fractal aggregates and calculated their $MAC_{BC,core\text{-}shell}$ values using the Lorenz-Mie theory (figure 4). Climate models typically assume core-shell morphologies to account for internal mixing of BC and apply the computationally inexpensive Mie theory to calculate their optical properties [6,7,12]. Unlike fractal aggregate morphologies, ρ for core-shell homogeneous spheres crosses over from the Rayleigh ($\rho < 1$) to the Geometric optics (GO) limit ($\rho > 1$) at diameters 100 – 300 nm for λ = 405 – 880 nm, respectively. Once in the GO regime, the amount of light penetrating into a spherical BC core is determined by its optical skin depth [34,35]. This effect is clearly visible when mapping the internal absorption fields of an aggregate and its equivalent core-shell model (figure 4 A-F). As the core diameter $D_{eq,BC}$ increases, the ratio $\frac{D_{eq,BC}}{Skin\ Depth}$ increases linearly to values between 1 and 6 indicating significant screening of light by the core's interior. The consequences of this photon screening is underestimation of MAC_{BC} values using the core-shell model, although it is noteworthy that the model has been shown to predict $E_{MAC_{BC}}$ values in good agreement with observational findings [29,30].

In summary, we present the first empirical evidence of light absorption by atmospheric BC demonstrating universal patterns and simple scaling laws. Our major findings are summarized in Table 1. Scaling behaviors represent universal concepts that underlie non-equilibrium physical systems such as aerosols, and hold great promise to serve as

computationally inexpensive parameterizations in climate models and satellite retrieval algorithms toward improving the accuracy of radiative forcing predictions. Based on insights gained from field studies, we speculate our scaling relations to be particularly applicable to accurately describing and modeling the optical properties of biomass burning aerosols in fresh- and moderately-aged conditions [28,36].

Use of the core-shell approximation has been suggested to introduce up to 50% uncertainty in modeled DRF by BC [9]. Via this study, we hope to convince the atmospheric aerosol community to refrain from using this approximation, especially for estimating MAC_{BC} of internally-mixed BC population. If use of this approximation is inevitable, then care must be taken to properly integrate the correction factor due to the optical skin depth of the BC core. Finally, we anticipate future laboratory and field studies to further refine these scaling laws, especially for unique case scenarios, such as BC core with absorbing coating materials, non-uniform distribution of coating mass and inclusions on a core, and a core with mass fractal dimension approaching 3 [37]. As part of this study, we performed sensitivity analysis by assigning a weakly absorbing imaginary index ($\approx 5 \times 10^{-2}$) to the OC coating at 405 nm, representative of brown carbon. The deviations in scaling dependencies of $E_{MAC_{BC}}$ could be considered as negligible, but MAC_{BC} values showed considerable deviations from the observed scaling dependencies.

Y	Y_0	S	β
$E_{MAC_{BC}}$	1	$\frac{M_{total}}{M_{BC}}$	$1/3$
MAC_{BC}	$\frac{3.6}{\lambda}$	$\frac{M_{total}}{M_{BC}}$	$1/3$
	$3.6\left(\frac{M_{total}}{M_{BC}}\right)^{1/3}$	λ	-1

$\frac{MAC_{BC}}{MAC_{BC,Core-Shell}}$	$0.55 - 0.80$	$\frac{D_{eq,BC}}{Skin\ Depth}$	$^3/_4$

Table 1: Summary of Power-Law scaling relations of the form $Y = Y_0 S^{\beta}$ for key light absorption parameters of internally-mixed BC aerosol.

Acknowledgements: This work was supported by the U.S. National Science Foundation (AGS-1455215, CBET-1511964, and AGS-PRF-1624814) and the National Aeronautics and Space Administration Radiation Sciences Program (NNX15AI66G) managed by Dr. Hal Maring. The authors thank an anonymous reviewer for insightful comments, and Drs. Dantong Liu and James Allen of University of Manchester for sharing of the raw data from their field experiments.

REFERENCES:

[1] T. Bond *et al.*, J. Geophys. Res., **118**, 5380 (2013).

[2] V. Ramanathan and G. Carmichael, Nat. Geosci. **1**, 221 (2008).

[3] Ö. Gustafsson and V. Ramanathan, Proceedings of the National Academy of Sciences **113**, 4243 (2016).

[4] O. Boucher *et al.*, Proceedings of the National Academy of Sciences, 201607005 (2016).

[5] T. F. Stocker, Q. Dahe, and G.-K. Plattner, Working Group I Contribution to the Fifth Assessment Report of the Intergovernmental Panel on Climate Change. Summary for Policymakers (IPCC, 2013) (2013).

[6] M. G. Flanner, C. S. Zender, J. T. Randerson, and P. J. Rasch, J. Geophys. Res., **112** (2007).

[7] Q. Wang *et al.*, J. Geophys. Res., **119**, 195 (2014).

[8] S. China, C. Mazzoleni, K. Gorkowski, A. C. Aiken, and M. K. Dubey, Nature Communications **4** (2013).

[9] S. Liu *et al.*, Nature communications **6** (2015).

[10] C. D. Cappa *et al.*, Science **337**, 1078 (2012).

[11] J. Peng *et al.*, Proceedings of the National Academy of Sciences **113**, 4266 (2016).

[12] M. Z. Jacobson, Nature **409**, 695 (2001).

[13] D. Liu *et al.*, Nat. Geosci. **10**, 184 (2017).

[14] S. H. Chung and J. H. Seinfeld, J. Geophys. Res., **110** (2005).

[15] W. R. Heinson, P. Liu, and R. K. Chakrabarty, Aerosol Sci. Technol. **51**, 12 (2017).

[16] B. J. Turpin and H.-J. Lim, Aerosol Sci. Technol. **35**, 602 (2001).

[17] M. Hess, P. Koepke, and I. Schult, Bulletin of the American Meteorological Society **79**, 831 (1998).

[18] M. A. Yurkin and A. G. Hoekstra, Journal of Quantitative Spectroscopy and Radiative Transfer **112**, 2234 (2011).

[19] T. Bond and R. Bergstrom, Aerosol Sci. Technol. **40**, 27 (2006).

[20] C. H. Jung, H. J. Shin, J. Y. Lee, and Y. P. Kim, Atmosphere **7**, 65 (2016).

[21] H. Horvath, Atmos. Environ. **27**, 293 (1993).

[22] P. DeCarlo *et al.*, Atmos. Chem. Phys. **7**, 18269 (2007).

[23] G. Saliba *et al.*, Aerosol Sci. Technol. **50**, 1264 (2016).

[24] M. Hallquist *et al.*, Atmos. Chem. Phys. **9**, 5155 (2009).

[25] T. Moise, J. M. Flores, and Y. Rudich, Chem. Rev. (Washington, DC, U. S.) **115**, 4400 (2015).

[26] R. C. Moffet, R. E. O'Brien, P. A. Alpert, S. T. Kelly, D. Q. Pham, M. K. Gilles, D. A. Knopf, and A. Laskin, Atmos. Chem. Phys. **16**, 14515 (2016).

[27] R. M. Healy *et al.*, J. Geophys. Res., **120**, 6619 (2015).

[28] A. Knox, G. Evans, J. Brook, X. Yao, C.-H. Jeong, K. Godri, K. Sabaliauskas, and J. Slowik, Aerosol Sci. Technol. **43**, 522 (2009).

[29] M. Shiraiwa, Y. Kondo, T. Iwamoto, and K. Kita, Aerosol Sci. Technol. **44**, 46 (2010).

[30] A. R. Metcalf, C. L. Loza, M. M. Coggon, J. S. Craven, H. H. Jonsson, R. C. Flagan, and J. H. Seinfeld, Aerosol Sci. Technol. **47**, 326 (2013).

[31] D. A. Lack, J. M. Langridge, R. Bahreini, C. D. Cappa, A. M. Middlebrook, and J. P. Schwarz, Proc. Natl. Acad. Sci. U. S. A. **109**, 14802 (2012).

[32] M. Gyawali *et al.*, Atmosphere **8**, 217 (2017).

[33] C. M. Sorensen, Aerosol Sci. Technol. **35**, 648 (2001).

[34] H. van de Hulst, New York: Dover, 1981 (1981).

[35] G. Wang, A. Chakrabarti, and C. M. Sorensen, JOSA A **32**, 1231 (2015).

[36] T. Ryerson *et al.*, J. Geophys. Res., **118**, 5830 (2013).

[37] Y. Wang *et al.*, Environmental Science & Technology Letters **4**, 487 (2017).

[38] See Supplemental Material [**url**], which includes Refs. [39-45].

[39] P. Meakin, J. Colloid Interface Sci. 102, 505 (1984)

[40] W. Heinson, C. Sorensen, and A. Chakrabarti, J. Colloid Interface Sci. 375, 65 (2012).

[41] M. A. Yurkin and A. G. Hoekstra, Journal of Quantitative Spectroscopy and Radiative Transfer 112, 2234 (2011).

[42] E. Zubko *et al.*, Appl. Opt. 49, 1267 (2010)

[43] D. Fry, A. Mohammad, A. Chakrabarti, and C. Sorensen, Langmuir 20, 7871 (2004).

[44] C. F. Bohren and D. R. Huffman, J Wiley & Sons, New York (1983).

[45] N. V. Voshchinnikov, G. Videen, and T. Henning, Appl. Opt. 46, 4065 (2007).